

Spectral Dependences of the Atmospheric Aerosol Optical Depth in the Extended Spectral Region of 0.4-4 μm

S.M. Sakerin and D.M. Kabanov
Institute of Atmospheric Optics
Tomsk, Russia

Introduction

Regular measurements of the aerosol optical depth (AOD) in different regions are important for studying the aerosol climate forcing (see Report WMO 2005; Holben 1998). To date, the majority of measurements of AOD - $\tau^A(\lambda)$ are carried out in the relatively narrow wavelength range 0.34-1 μm , where the effect of aerosol on the radiative processes is more significant than molecular absorption. To obtain a more accurate definition of the climatic role of atmospheric aerosol, it is necessary to obtain data in different regions and in a wider wavelength range of the incoming radiation. The results in the longwave (LW) range (more than 1 μm) are represented now by short cycles of measurements of AOD in some regions (Shiobara 1996; Vitale 2000). The peculiarities of the spectral dependence of AOD in the wavelength range $\sim 0.4\text{-}4 \mu\text{m}$ are discussed in this paper on the basis of long-term observations in the region of Tomsk.

Characteristics of Experiments

Tomsk is situated in the southern part of Western Siberia. The atmosphere in this region is weakly subjected to industrial impact and is the typical region of boreal climatic zone. Measurements of the atmospheric transparency were carried out by means of sun photometers in suburb area of Tomsk. Observations in the first period (1992-1999) were carried out mainly in summer in the shortwave (SW) range 0.37-1.06 μm . Since 2000, measurements of $\tau^A(\lambda)$ became all-the-year-round and were added by measurements in the "transparency windows" of the atmosphere in the LW range 1.2-4 μm . Specifications of the photometer (Kabanov 2001), used during the last period are presented in Table 1.

Table 1. Main parameters of the sun photometer.		
Characteristics	SW channel	LW channel
Field of view, $^\circ$	1,38	1,48
Filter passband, μm	0,37; 0,41; 0,44; 0,48; 0,50; 0,55; 0,67; 0,87; 0,94; 1,05	1,25; 1,55; 2,20; 3,97
Filter FWHM, μm	0.005-0.012	0.015-0.04
Time of one cycle, s	50	

To retrieve AOD from the atmosphere in the infrared wavelength range, the technique (Kabanov 1997) was developed, which takes into account the molecular absorption of gases and the real variability of the water vapor content. The molecular absorption is removed at the first step by means of dividing the measured signals of the atmospheric transparency to the transmission functions of the gaseous components. The gas absorption functions were calculated using the LOWTRAN-7 spectral data for the real light-filter transmission contours. The data of radiation extinction in the absorption band of $0.94 \mu\text{m}$ were attracted to take into account the variability of the columnar water vapor of the atmosphere. According to our estimates, the error in determining AOD in the SW range is 0.01-0.02, and can reach 0.02-0.03 in the infrared range.

Measurements obtained before 2000 were performed in separate 5-30 min long series, when clouds had not covered the sun. After passing to automated regime of all-the-year-round measurements, the procedure of detecting the “cloudless sun” situations was performed using the special software (Kabanov 2001). In addition, filtering data on the effect of clouds (cloud screening) was performed. The daily and hourly mean values of AOD with reference to the local time were used for analysis. The total number of days during the measurement period (23.05.92 – 04.10.05) was 1139, and 6444 hourly mean values. The total number of days in the post-volcanic period (after 1995) is 1019, and 5708 hourly mean values. The results obtained in summer in the wavelength range $0.37\text{-}1.06 \mu\text{m}$ are the most full.

Taking into account experimental studies of AOD in the LW range, model estimation of the spectral dependences of the aerosol extinction was performed, which is physically possible for the typical distributions of the aerosol microstructure and the values of the refractive index. Calculations by the Mie theory were conducted using the standard software for three optically active aerosol fractions: fine ($r < 0.4 \mu\text{m}$), intermediately dispersed ($0.4 < r < 1 \mu\text{m}$), and coarse ($r > 1 \mu\text{m}$). The model estimates show the following:

- spectral dependence of the extinction of radiation by fine particles is characterized by a power decrease with wavelength and extends to $1\text{-}1.5 \mu\text{m}$
- extinction of radiation by coarse aerosol is constant in the wavelength range up to $\sim 1 \mu\text{m}$, and then small increase of extinction can be observed
- the spectral dependence of extinction of particles of intermediate size ($0.4 < r < 1 \mu\text{m}$) combines the peculiarities of both aforementioned fractions: weakly pronounced minimum is observed in SW range at $0.6\text{-}0.8 \mu\text{m}$, then monotonous decrease follows.

As for the spectral dependence of the total extinction of all three aerosol fraction, one can draw the following conclusions:

- the degree of selectivity $\tau^A(\lambda)$ in SW range depends on microphysical characteristics of fine particles and on the ratio of the optical contributions of fine and coarse aerosol;

- “interwave” deviations of up to ~0.2 can be observed in the LW range. This is comparable with the error in determining AOD.

Results

Spectral Dependence of AOD in SW Range

The Angstrom formula is usually used for quantitative characterization of the spectral dependence $\tau^A(\lambda)$ in SW range:

$$\tau^A(\lambda) = \beta \cdot \lambda^{-\alpha}, \quad (1)$$

where α is the index of selectivity (Angstrom exponent), $\beta \approx \tau^A(1 \mu\text{m})$ is the turbidity coefficient. The parameter β is close to the value of AOD in LW range and approximately characterizes the content of coarse particles.

Figure 1 shows that mean dependences of AOD in different atmospheric situations are well described by Eq. (1). Maximum selectivity $\tau^A(\lambda)$ and the value of the exponent $\alpha=1.75$ are characteristic of the forest fire events, and minimum values were observed in winter and after Mt. Pinatubo eruption ($\alpha=0.87$). Figure 2 shows the effect of the ratio of the optical contributions of two aerosol fractions on α . The tendency to decrease α as β increases is shown. That means, the index α depends partially on the value β , or on the content of coarse particles. The maximum values α (up to 2.5) are observed at $\beta < 0.02$, when the content of coarse fraction has been minimum, and the maximum values α at $\beta > 0.16$ become less than 1.

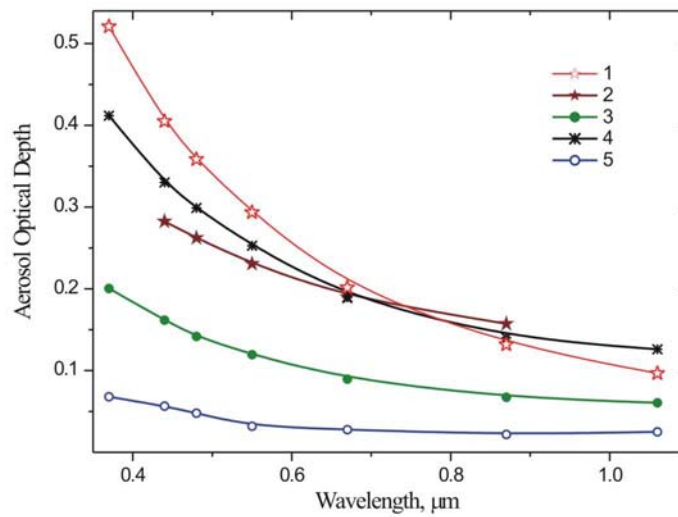


Figure 1. Mean $\tau^A(\lambda)$ in different situations: (1) during fires; (2) after the Mt. Pinatubo eruption (summer 1992); (3) the entire data array (1992-2005); (4, 5) under conditions of low and high atmospheric turbidity (which are not included into 90% of the most probable values τ^A).

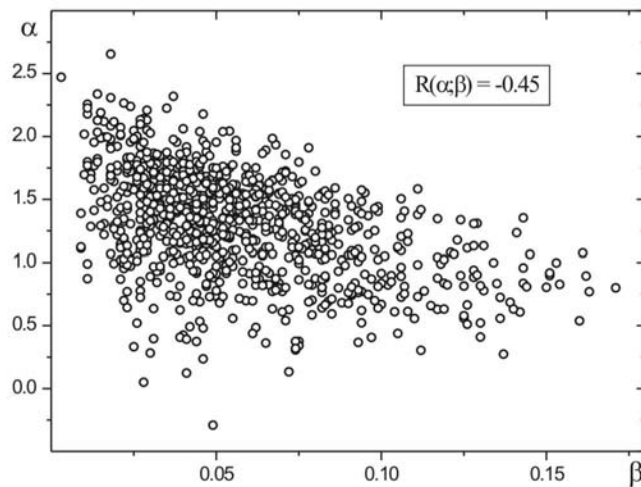


Figure 2. Scattering diagram of the values α and β (data array of 1995-2005).

Figure 3 gives the general image of interannual variability of AOD and the index of selectivity α during the entire period of measurements. The long-term variability was estimated using only the summer data, when the longest series are available. The change of the characteristic in the initial period (1992-1994), and in other regions of the earth, was caused by consequences of the Mt. Pinatubo eruption – decrease of

AOD and increase of α . Mean value $\tau^A(0.55)$ after cleaning of the atmosphere varied in the range 0.08-0.15. Decrease of variations and small increase of AOD are observed last 5 years. As for variations of the parameter α in after-volcanic period, its decrease was observed several first years with minimum in 1996, and then it stabilized at the level of ~ 1.5 . The following conclusions can be drawn on the basis of the histograms of distributions of the characteristics (Figure 4):

- principal ranges of variations (90%) are the following: $\tau_{0.55}^A=0.04-0.23$, $\alpha=0.53-1.94$, $\beta=0.02-0.09$;
- the most probable values (modes) are 0.09, 1.55 and 0.045, respectively.

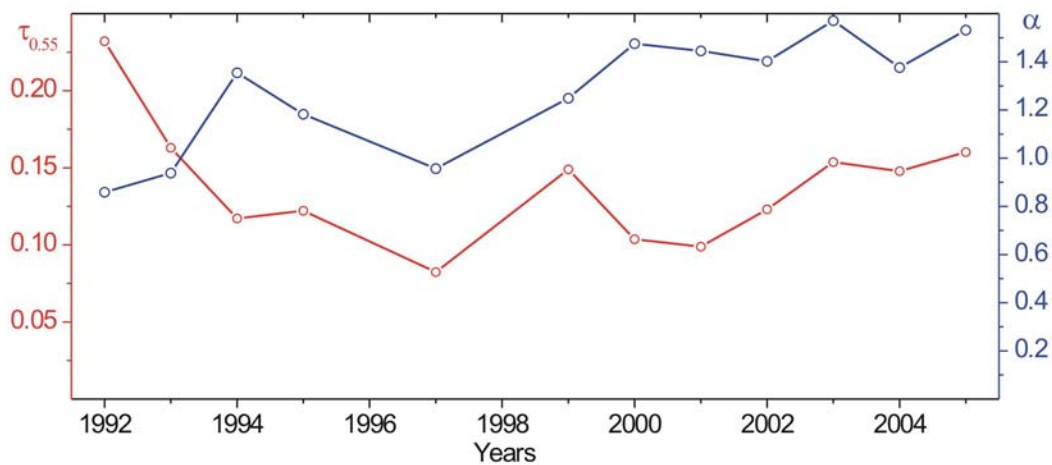


Figure 3. Interannual variability of $\tau^A(0.55)$ and the index α in summer.

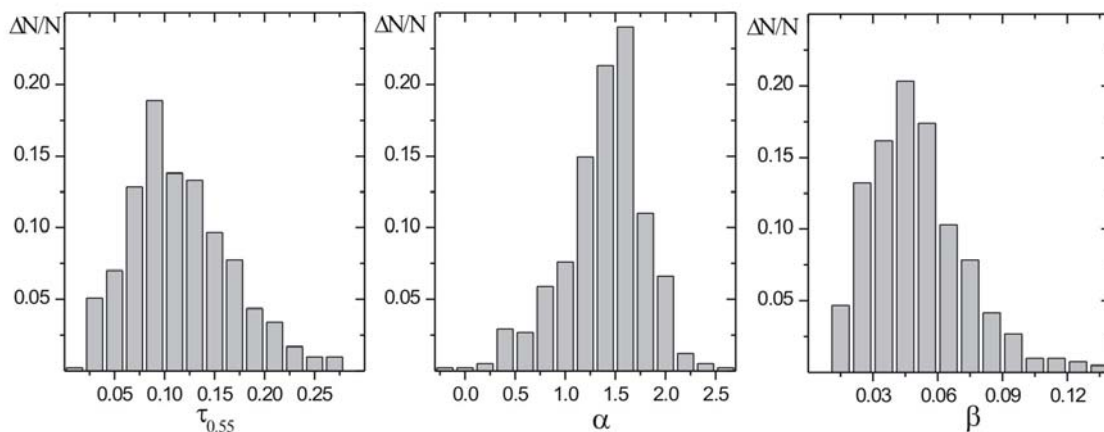


Figure 4. Histograms of the distributions of $\tau_{0.55}^A$, α and β (summer 1995-2005, except fires).

To determine annual peculiarities, classification was made according to seasons, air masses – continental arctic and continental polar. The separation on seasons was conducted on calendar terms. The mean values for these conditions are presented in Table 2 and Figure 5. The situations of forest fires, which are typical for the boreal zone in summer, are selected as a separate class. Hourly mean values $\tau^A(\lambda)$ were used for analysis of these data because of their less quantity.

	Winter	Spring	Summer	Autumn	Fire (summer)	Volcano (summer 1992)	Total		Summer	
							Ca	Cp	Ca	Cp
$\tau^A(0.55)$	0.142	0.145	0.116	0.095	0.283	0.232	0.114	0.121	0.104	0.116
α	1.06	1.28	1.39	1.26	1.75	0.86	1.29	1.34	1.34	1.435
β	0.079	0.071	0.050	0.046	0.098	0.138	0.055	0.056	0.047	0.049
$\bar{\tau}_c$	0.067	0.067	0.050	0.037	0.072	-	-	-	-	-

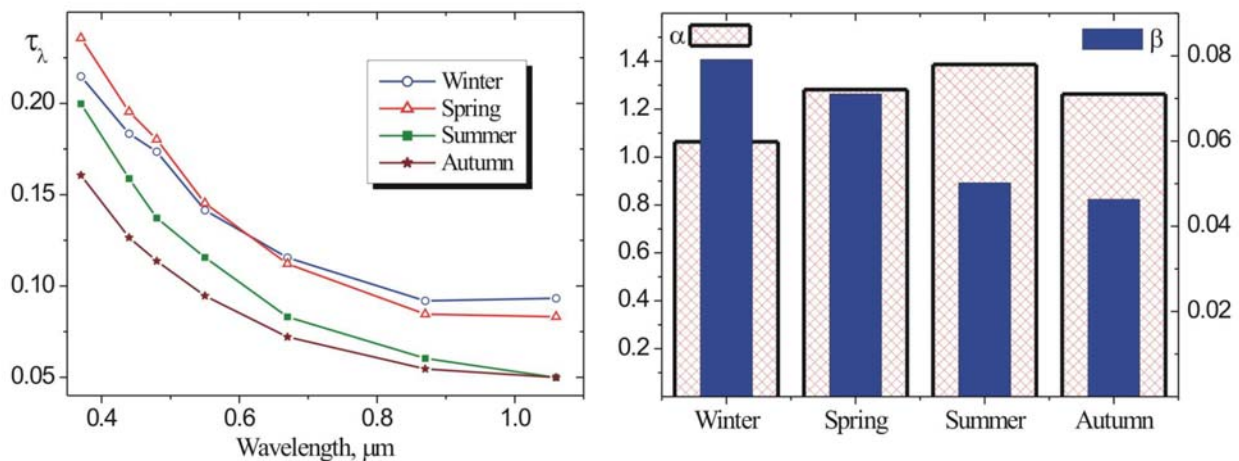


Figure 5. Seasonal variations of the mean values of $\tau^A(\lambda)$, α and β .

It is revealed that fall season strongly differs from spring and winter by total turbidity of the atmosphere. Besides, individual peculiarities of α and β are observed in different seasons:

1. minimum values α (i.e. selectivity of AOD) and, simultaneously, maximum values β (i.e. the content of coarse particles) are characteristic of winter;
2. spring is characterized by quite great, but not maximum values α and β ;
3. maximum α and relatively small β are characteristic of summer;
4. the value β in fall is minimum, and the index α is close to its annual mean value.

The revealed seasonal peculiarities are observed not only in the index of selectivity, but also in different combinations of the values α and β . Seasonal variations of α occurs partially under the effect of variations of the parameter β . Another situation is observed when comparing AOD in different air masses (Figure 6). The values of $\tau^A(\lambda > 0.6 \mu\text{m})$ and the parameter β , which are mainly determined by the content of local coarse aerosol, are practically the same in continental arctic and continental polar air masses. So the differences in α and $\tau^A(\lambda > 0.6 \mu\text{m})$ are caused mainly by fine aerosol, the content of which is less in arctic air. Qualitatively analogous result is obtained when comparing AOD in different air masses in the entire data array (see Table 2).

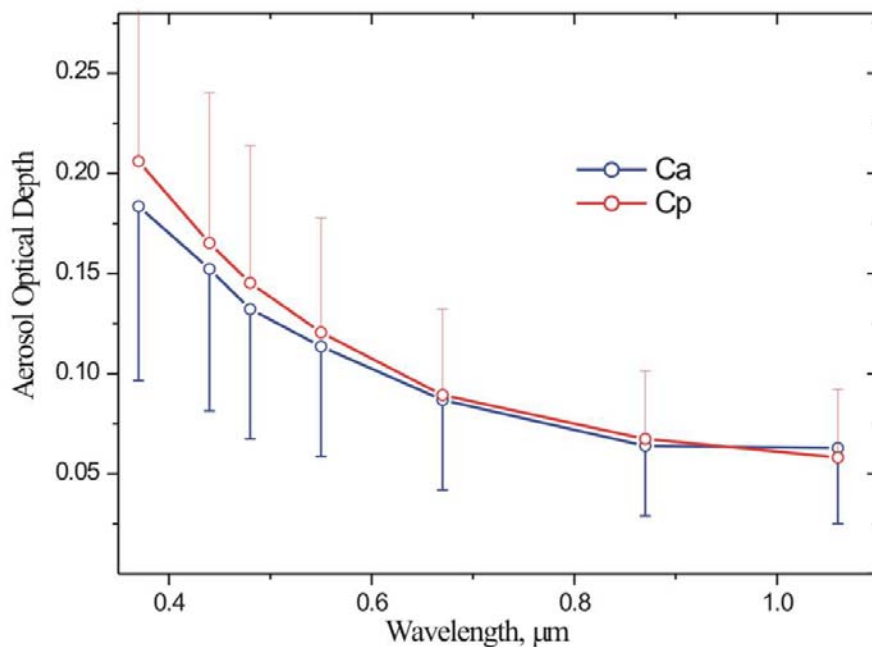


Figure 6. Mean $\tau^A(\lambda)$ in two types of air masses.

In general, one should note that the differences in the characteristics $\tau^A(\lambda)$ in different seasons and air masses in the background region of Siberia is not so great as is observed in other regions. The characteristics of AOD during forest fires strongly differ from other atmospheric situations (Figures 7 and 8). Great content of namely fine particles is usually observed in forest fire smokes that lead to the increase of α . In our case, the increase of the concentration of particles was observed in the size range of coarse fraction too (approximately twice increase of β).

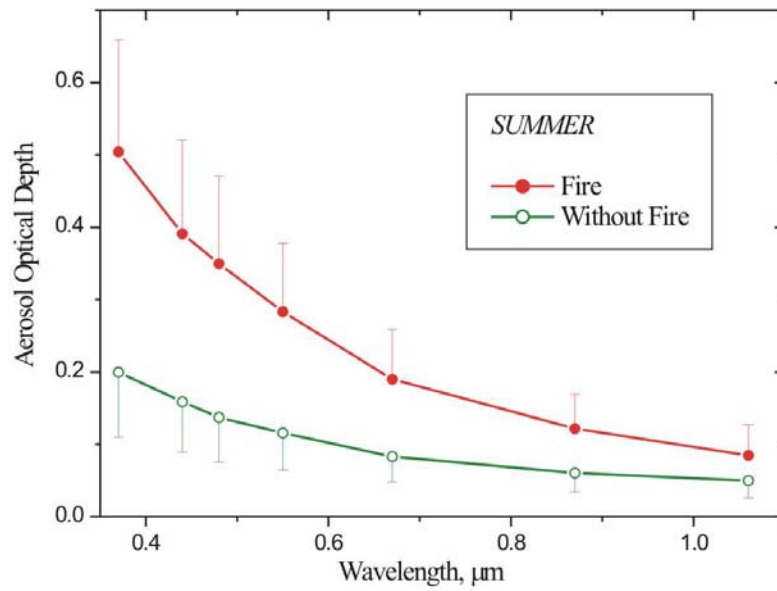


Figure 7. Mean $\tau^A(\lambda)$ during forest fires and under clean conditions.

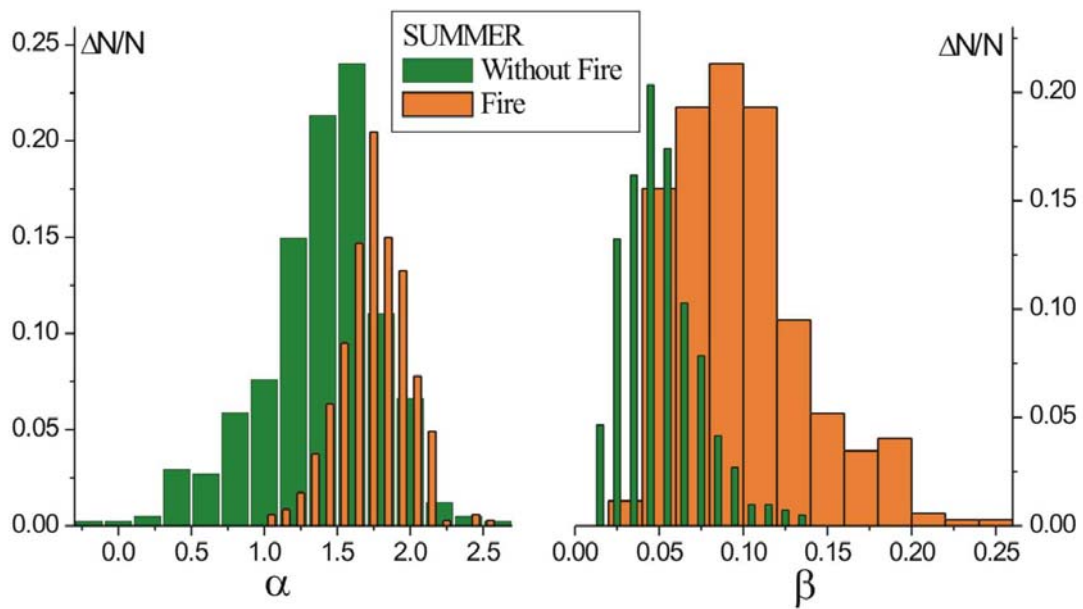


Figure 8. Histograms of α and β during forest fires and under clean conditions.

Spectral Dependence in LW Range

Measurements of $\tau^A(\lambda)$ in a wider wavelength range (up to 4 μm) were performed only last years, and the quantity of data is smaller. Nevertheless, mean characteristics in SW range are in good agreement with the data of the longer series of observations (see Figures 9 and 5). Mean dependence $\tau^A(\lambda)$ for the entire data array in LW range is smooth, the power decrease gradually passes (in the range 0.8-1.5 μm) to neutral behavior with mean value of 0.052. To estimate seasonal differences, mean values AOD in the range 1.2-4 μm were calculated (see $\bar{\tau}c$ in Table 2). The maximum level of $\bar{\tau}c$ (and the content of coarse particles) is observed during the events of forest fires and in spring-winter period, and minimum is observed in fall. The values AOD in summer are intermediate with tendency of increase AOD when approaching to 4 μm .

Mean value of the “interwave” deviations of AOD ($\tau_{max} - \tau_{min}$) in LW range is about 0.02. The differences of AOD in two wavelength ranges $\Delta_{1-2} = \tau^A(1 \mu\text{m}) - \tau^A(2.2 \mu\text{m})$ и $\Delta_{2-4} = \tau^A(2.2 \mu\text{m}) - \tau^A(4 \mu\text{m})$ were considered for more detailed estimation of the peculiarities of the behavior of $\tau^A(\lambda)$. It is seen in Figures 9 and 10, than the difference in the first range (up to 2.2 μm) is usually positive, that means, the decrease of AOD is observed, and the annual mean value Δ_{1-2} is ~ 0.01 . Mean annual dependence of $\tau^A(\lambda)$ in the range 2.2-4 μm is neutral, but cold season differs from warm. A small increase of AOD when approaching 4 μm is observed from May to October, and the decrease of AOD is observed in cold season. The rate of the decrease is the same, in average, and in the range before 2.2 μm .

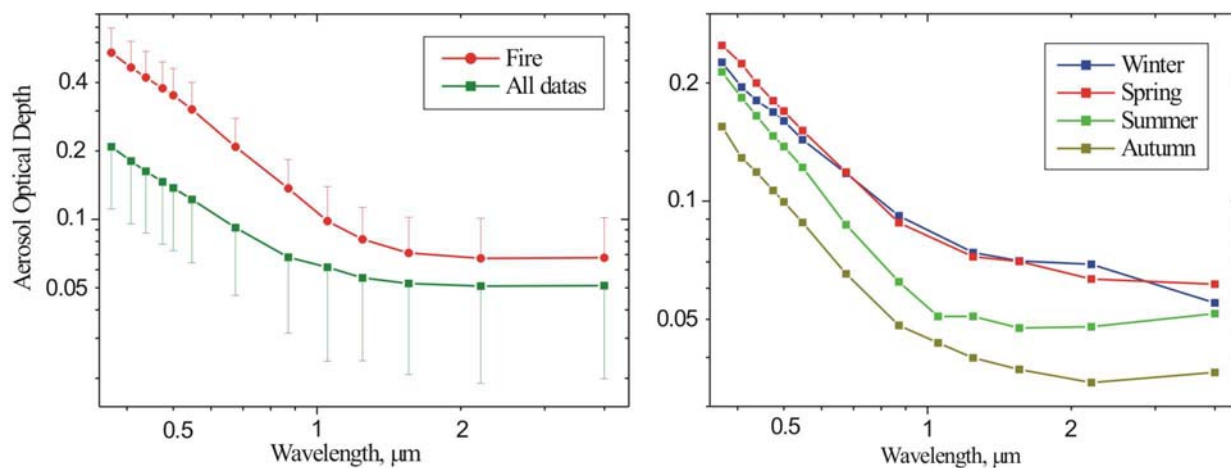


Figure 9. Mean dependences $\tau^A(\lambda)$ in the wide wavelength range.

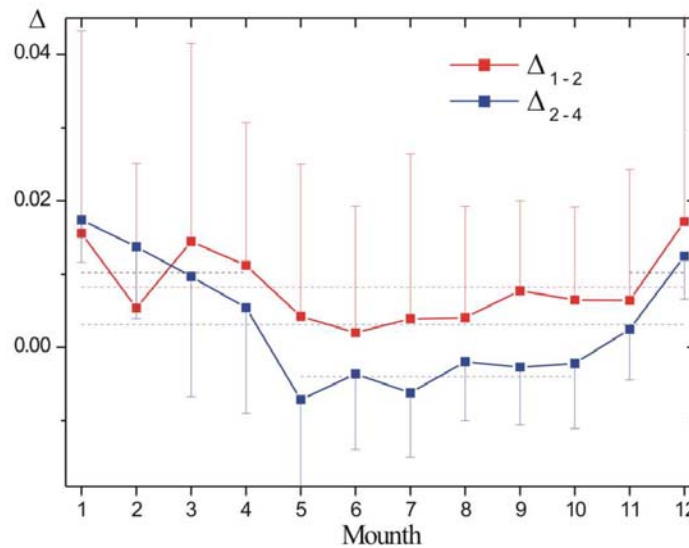


Figure 10. Inter-month variability of Δ_{1-2} and Δ_{2-4} .

Taking into account closeness of β and $\bar{\tau}_c$ (see Table 2), the possibility was analyzed of estimation of the mean level of AOD in LW range using the values β . The results shown in Figure 11 are evidence of the fact that close linear correlation between these two parameters is observed (the correlation coefficient is 0.853): $\bar{\tau}_c \approx 0.06 + 0.807 \cdot \beta$. Thus, it is possible to approximately determine $\bar{\tau}_c$ from the results of measurements of AOD in SW range.

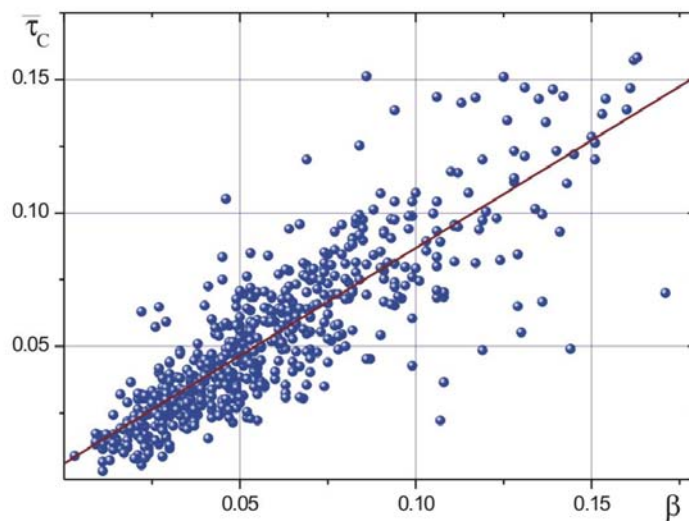


Figure 11. Correlation between β and $\bar{\tau}_c$.

Acknowledgments

The work was supported by the Atmospheric Radiation Measurement Program (Contract No. 5012) and the Russian Foundation for Basic Research (grant No. 05-05-64410).

Corresponding Author

Sergey M. Sakerin, sms@iao.ru

References

Holben, BN, TF Eck, I Slutsker, D Tanre, JP Buis, A Setzer, E Vermote, JA Reagan, YJ Kaufman, T Nakadjima, F Lavenu, I Jankowiak, and A Smirnov. 1998. "AERONET – A federated instrument network and data archive for aerosol characterization." *Remote Sensing Environment* 66(1)1-16.

Kabanov, DM, and SM Sakerin. 1997. "Some problems in determining optical thickness of the atmosphere due to extinction by aerosol in the near IR." *Atmospheric and Oceanic Optics* 10(08)540.

Kabanov DM, SM Sakerin, and SA Turchinovich. 2001. "Sun photometer for scientific monitoring (instrumentation, techniques, algorithms)." *Atmospheric and Oceanic Optics* 14(12)1067-1074.

Report (No 162) WMO/GAW expert's workshop on a global surface-based network for long term observations of column aerosol optical properties. 2005. WMO TD No. 1287, Davos, Switzerland, 144p.

Shiobara, M, JD Spinhirne, A Uchiyama, and S Asano. 1996. "Optical depth measurement of aerosol, cloud, and water vapor using sun photometers during FIRE Cirrus IFO II." *Journal of Applied Meteorology* 35:36-46.

Vitale V, C Tomasi, A Lupi, A Cacciari, and S Marani. 2000. "Retrieval of columnar aerosol size distributions and radiative-forcing evaluations from sun-photometric measurements taken during the CLEARCOLUMN (ACE 2) experiment." *Atmospheric Environment* 34:5095-5105.